

Article

Impact of Shear Zone on Rockburst in the Deep Neelum-Jehlum Hydropower Tunnel: A Numerical Modeling Approach

Abdul Muntaqim Naji ¹, Hafeezur Rehman ¹, Muhammad Zaka Emad ², and HanKyu Yoo ^{1,*}

¹ Department of Civil and Environmental Engineering, Hanyang University, 55 Hanyangdaehak-ro, Sangnok-gu, Ansan, 426-791, Republic of Korea.

² Department of Mining Engineering, University of Engineering and Technology, Lahore, Pakistan.

*Correspondence: hankyu@hanyang.ac.kr; Tel. 82-31-400-5147; Fax: 82-31-409-4104

Abstract: Rockburst is a hazardous phenomenon in deep tunnels influenced by geological structural planes like faults, joints, and shear planes. Small-scale shear-plane-like structures have damaging impact on the boundaries of the tunnel, which accumulate high stresses. Such a shear plane was exposed in the side wall of the right headrace tunnel in the Neelum-Jehlum Hydropower Project. This project is constructed in the tectonically active Himalayas with high stress conditions. A shear plane combined with high stress conditions is very dangerous in deep excavations. The influence of a shear zone on rockburst occurrence near a tunnel is studied. The FLAC3D explicit code simulated the shear zone in the right tunnel, revealing that the stresses are concentrated near the shear zone, with no stress concentration in the left tunnel, which has neither shear zone nor rockburst. Rock mass was displaced near this shear zone even before excavation. Modeling results confirm that the side wall shear zone of the tunnel has a major influence on rockburst occurrence. A shear slip along this plane released huge amounts of energy, causing human fatalities and property damage. A numerical simulation validates the actual conditions and helps us understand the phenomenon of stress concentration near the shear zone and its impact during deep tunneling.

Keywords: deep tunnel, high stresses, shear zone, rockburst, energy released

1. Introduction

Rock burst is one of the most hazardous phenomena which intensify during construction of deeper excavations. It can be caused by either brittle failure or slippage along structural planes in deep hard rock [1]. Rockburst results in a sudden or violent damage to an excavation, usually associated with seismicity due to huge energy accumulation [2]. It not only causes damage to equipment and machinery, but also to nearby structures. A lot of research work has been done to find the mechanism of rockburst in mining [3-5].

7]. However, this phenomenon is not much studied in civil tunneling for hydropower and road projects. A few hard rock tunnels have experienced intensive rockbursts worldwide. This includes the Jinping hydropower tunnels in China, the Neelum-Jhelum Hydropower Project (NJHPP) twin headrace tunnels (right and left) in Pakistan, and the Gotthard base tunnel in Europe [8-11]. Kaiser and Cai [12] identified four different factors that cause rockburst failure: geotechnical, geological, mining, and seismic. Different studies have been done to understand the effect of these factors on rockburst damage [13-15]. We focus here on the geological factor, which includes geological studies of the area and the influence of geological structures (faults, shear zones, anticline, and synclines) on the occurrence of rockburst.

The stress magnitude around an opening usually increases with increased depth and geological structures have a strong influence on the in situ stress orientation [16]. Shepherd, Rixon [17] have effectively reviewed rock mechanics of rockburst in presence of different geological structures including Thrusts, strike-slip faults and recumbent fold hinges. Usually, during deep civil tunneling, geological weaknesses like faults or shear zones are found nearby, which causes unfavorable and complex stress scenario. The stresses are usually concentrated near these structures, which results in large deformations and failure processes because rock masses with discontinuities, e.g., joints, dykes, bedding planes, and shear zones, may fail when the shear stress overcomes the shear strength of the discontinuities (Ryder 1988). Hedley [18] worked on Ontario hard rock mines and found that the underground mines are prone to bursting when geological discontinuities are nearby. Ortlepp and Stacey [19] explained five different mechanism behind rockbursts in deep mines: strain burst, buckling, face crushing, virgin shear, and reactivated shear in existing faults. Rockburst occurs due to shear failure along weak planes (pre-existing faults or shear zones,) within the rock mass. Durrheim, Roberts [20] found regional structures as a source mechanism during the investigation of 21 rockburst cases in deep South African gold mines. Sudden ejection of previously intact rock in a massive rock mass may be induced by fault slip or shear rupture [21]. The presence of faults and joints were the main reason behind the rockburst events of the pilot tunnels of the Jinping II hydropower project in China [22]. Snelling, Godin [23] worked at the Creighton Mine, Canada and found that geological structures resembling shear zones experiences frequent micro-seismic and often macro-seismic events. More than 20 rockburst events associated with structural planes have been listed during the construction of the Jinping-II headrace tunnels [24]. These structure planes become barriers to stress adjustment in surrounding rock mass in deep tunnels. This leads to concentration of tangential stress between the excavation boundary and structural plane along with huge amount of accumulated energy [14]. Laboratory test were conducted to explain about structure type rockburst for three possible rockburst mechanisms. It

was found that small-scale structural planes were main controlling factors for rockburst [10]. Manouchehrian and Cai [25] used the Abaqus2d explicit code to explain the role of discontinuities around tunnels during rockburst and confirmed that more violent rockburst occurs in the presence of geological structures.

A rockburst surrounding a structural plane is more destructive than one that is not surrounded by any structural plane [14]. Civil engineering tunnels are influenced by small structure planes, whereas deep mines have faults or discontinuities that usually are tens or hundred meters long. These small-scale structures can easily be reactivated when they are present in the vicinity of a tunnel and shear failure occurs. These planes played a very important role for the intense rockburst during the construction of the Jinping-II hydropower project (NJHPP). Mechanism of intense rockbursts induced by a nearby shear zone in deep hydropower tunnels is still unclear and which needs further studies. In this paper, the most intense rockburst of May 31, 2015, which occurred in the right headrace tunnel of the Neelum-Jehlum Hydropower Project is studied. It is believed that a shear plane exposed in the wall of the headrace tunnel was a favorable condition for a rockburst to trigger. We use a FLAC3D numerical simulation to investigate the mechanism of shear-zone-type rockburst. We also compare the results between the twin headrace tunnels where a shear zone is present only in the vicinity of the right tunnel.

2. Project Description

NJHPP is constructed in the north-east area of Pakistan. The construction started in 2008. The 28.5 km long headrace tunnel is constructed to divert the water from the Neelum River to an underground power house to produce 969 MW of electric power. The project is in the mighty mountains of the Himalayas which are considered as hub of high stresses which causes rockburst in hard rocks and squeezing weak rock. In addition, the presence of mixed geology and structures make it worse possible conditions for tunneling. Owing to tectonics, the area is highly folded and faulted. A major fault in the region, Main Boundary Thrust (MBT) is passing nearby the project area. The project site is present in an earthquake active zone and the 2005 Muzaffarabad earthquake occurred in this area and caused more than 75000 fatalities.

Mostly, the headrace tunnels in project are excavated with the drill and blast method and with a TBM (Tunnel Boring Machine) as a single tunnel and twin tunnels, respectively. The overburden was up to 2000 m, which has the potential of rock bursting in hard rock after evaluating with different empirical rockburst indexes [26-28]. The TBM-excavated twin tunnels had an initial center to center distance of 33 m before the

major rockburst event of May 31, 2015 in the project history. This distance was increased to 66 m to avoid further inter-tunnel pillar bursting.

3. Geological Settings of the Area and In-situ Stresses

The northward movement of the Indian plate in the Himalayan orogenic system has caused several thrust faults in the region, such as the Muzaffarabad fault due to high horizontal stress built up [29]. The headrace tunnels pass through areas having adverse folding and faulting with a series of anticlines and synclines structures, along with local faults and shear zones as shown in Figure 1. The bedding planes were normally perpendicular to the tunnel direction, which is a favorable condition for construction [30]. However, abnormal stress concentration caused the bedding planes to be oriented along the tunnel direction, posing a great threat to tunnel stability [31]. The entire project is excavated in the Muree formation of sedimentary origin with a stratigraphic sequence of alternative beds. These beds comprise sandstone, siltstone, and mudstone. Sandstone is the strongest rock unit, having an average uniaxial compressive strength (UCS) of 86 MPa with a stiffness of 32 GPa. This unit is thickly bedded and at places massive and blocky, that's why most of the rockburst events occurred in this rock. Siltstone has medium strength and is sometimes mixed with mudstone and shale. The average UCS of Siltstone is 66 MPa with stiffness of 23.1 GPa. Mudstone is the weakest rock unit of the Muree formation and has an average UCS of 42 MPa with stiffness of 12.6 GPa. This unit has much less potential for rockburst because of its very low strength, but this rock unit has exhibited a typical Himalayan squeezing phenomenon at some locations.

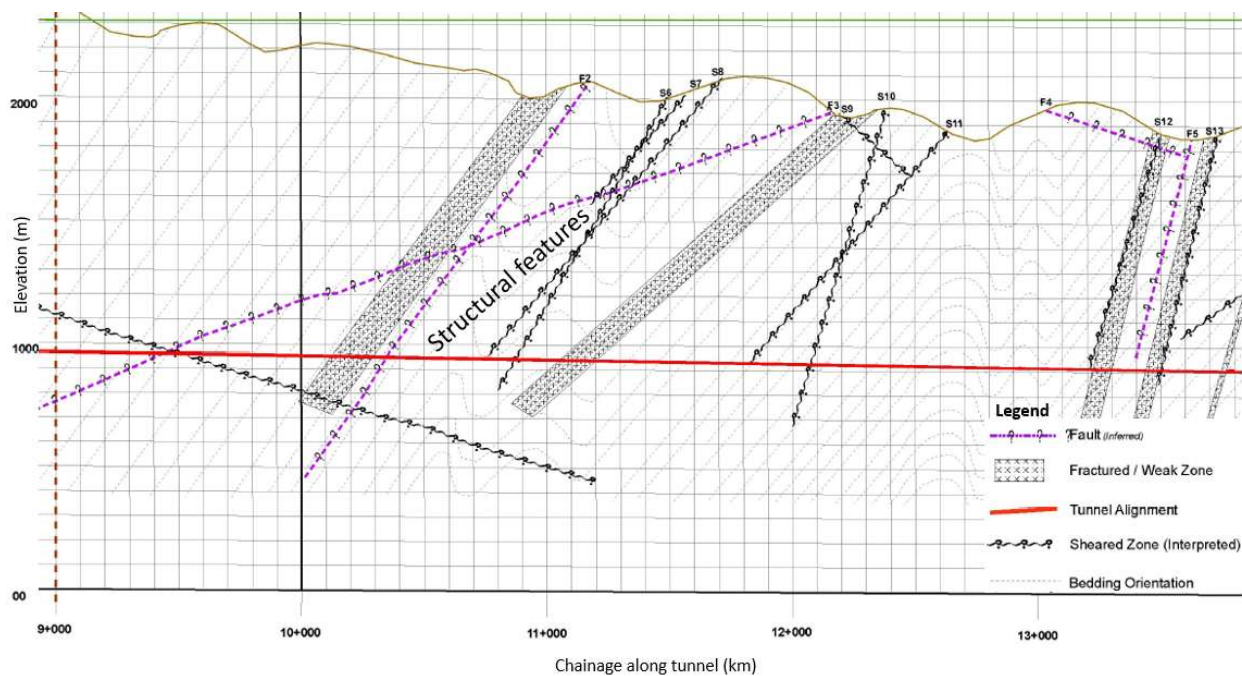


Figure 1. Geological map of the headrace tunnel area.

The engineering properties of these rocks are summarized in Table 1.

Table 1. GSI and intact rock parameters of different rock units along the headrace tunnel.

Rock Type	UCS (MPa)	GSI	E _i (GPa)	mi
Sandstone	86	65	32	17
Siltstone	66	50	23.1	7
Mudstone	42	50	12.6	9

Previous studies near the project area have witnessed high horizontal stresses due the active Himalayas [32]. In-situ stress measurements performed by over-coring in sandstone beds have also reflected high horizontal stresses in TBM tunnels. The value of the horizontal to vertical stress (K_0) was up to 2.9 as shown in Figure 2, where the major principal stress was oriented sub-horizontally and nearly perpendicular to the tunnel azimuth. This high value of K_0 has tectonic horizontal stress component which has increased principal horizontal stress caused frequent slabbing and rock bursting.

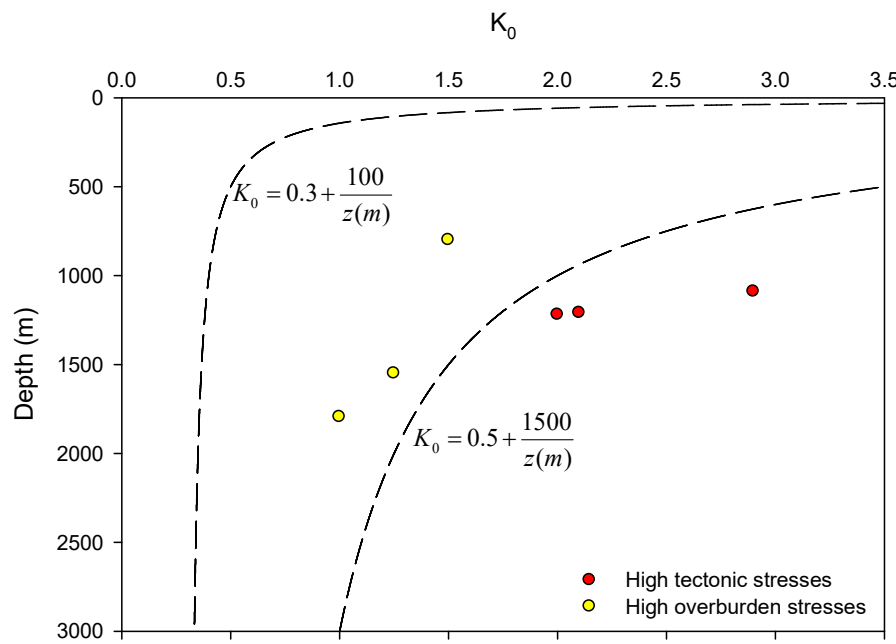


Figure 2. Measured horizontal to vertical stress ratio (K_0) at various depths, z (m).

Therefore, hard sedimentary rock under high stresses due to tectonics along a stress-concentrating synclinal structure, make the condition favorable for rockburst. Rockburst is empirically evaluated by rock brittleness and induced stress criteria [27, 33] based on rock strength and stresses at different locations.

4. Influence of Structural Planes on Rockburst in Deep Tunnels

During the excavation of deep tunnels, it is inevitable to encounter structural planes and most rockburst are influenced by these planes. They can be in the form of small scale joints or shear zones, which are usually, encountered during the excavation of hard rock tunnels in hydropower projects as compared to deep underground mining faces, which are mostly intercepted by large faults. Rockburst effected by these structures generally have higher intensities and produce more damage as compared to the ones that are not affected. These planes are sometimes visible on the boundary of the tunnel and sometimes present in the rock mass away from the boundary. These planes also control the bottom or lateral boundaries of the rockburst-damaged area [34]. The orientation of structural planes with tunnel axis and maximum principal stress is one of the main factors for rockburst intensity which can be categorized in the following different scenarios [24]. First, when the structural plane is at a large angle with the tunnel axis and the principal tangential stress, rockburst with high intensity and deep damage pit occurs at the footwall of the stiff structural planes. Second, a structural plane at a tunnel wall with a large angle with the tunnel axis and

small angle with the maximum tangential stress causes slight to moderate rockburst with moderate depth damage pit. Third, when it is parallel to the tunnel axis it causes high intensity rockburst with steep ridges and deep damage pit. Fourth, when the structural plane had a small angle with the tunnel axis and was passing near the tunnel boundary, causes intense rockburst with deep damage pit.

An extremely intense rockburst occurred in the Jinping-II hydropower tunnel, the structural plane had a small angle with the tunnel axis and was passing near the tunnel boundary, which caused an extremely intense rockburst with huge amounts of stored strain energy. Such rock bursts produce deep damage pits in the hanging wall area of the structural plane, which can be seen as a collapsed rock mass, as shown in Figure 3. In this type of rockburst, as the tunnel approaches, large amount of energy concentrated near the structural plane is released, which finally resulted in the deep damage pit. Presence of rigid structural planes sub-parallel to the axis of a deep hydropower tunnel was studied by Refs. [10, 35]. The huge amount of energy is accumulated and released, which resulted in the extremely intense burst on 28 November 2009, hereafter referred to as the “11.28” rockburst event in the drainage tunnel of the Jinping-II hydropower project, shown in Figure 3.

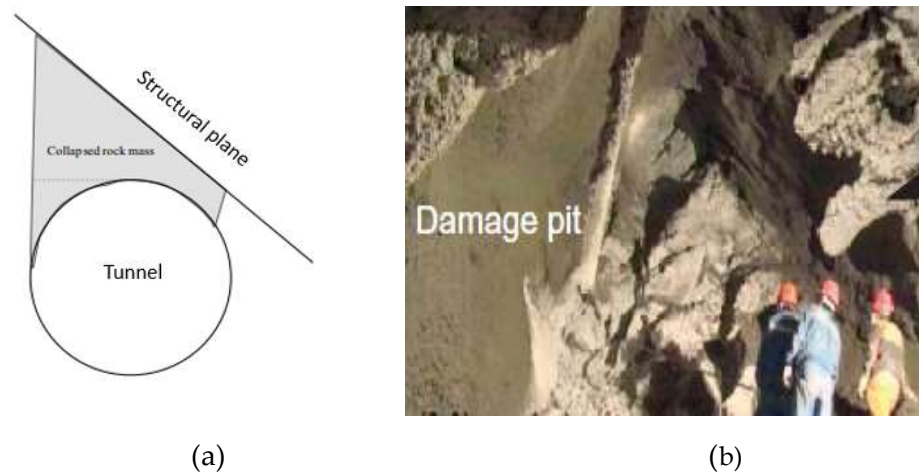


Figure 3. The “11.28” rockburst event caused by structural plane in Jinping-II drainage tunnel: (a) Schematic diagram and (b) damage pit

5. Impact of the Shear Zone on the Rockburst at NJHPP

In deep tunnels, rockburst is closely related to the geology and rock mechanics encountered. During deep tunnel excavation, geological and geo-mechanical failures are very critical. Information, either in the form of in-situ field measurements for in-situ stress or geological mapping is very important for revealing failure uncertainties. The shear zone can be at different locations like on the working face, near the vault, or on the side walls of the tunnel, having different angles with both the tunnel axis and maximum tangential stress. The presence of such a shear zone leads to a concentration of abnormal stress near these planes. The values of K_0 were out of range compared to the universally accepted depth vs K_0 plot, as shown in Figure 2. According to the geological mapping of the headrace tunnel, it passes many minor faults and shear planes, as shown in Figure 1. Two local faults, F2 and F3, and one shear zone is expected to pass the invert level at chainage 10+360 m and 9+350 m, respectively.

A prominent geological anomaly encountered during the tunnel excavation. The alternate beds of sandstone, siltstone, and mudstone experience high folding and faulting under high tectonic stresses. This complex geological setting resulted in unpredictable behavior of the excavation with frequent rockburst failure in the hard sandstone. The behavior of the hard sedimentary rock of the Murree Formation was further confirmed from exposure of a local shear plane (shown in Figure 4) in the drag-folded strata (as shown in Figure 5) near the right headrace tunnel boundary. The over-coring, in-situ stress measurement program, also confirmed a high horizontal stress regime in this chainage range. Thus, this anomalous region caused a series of strain burst failures due to stored strain energy before the main shear zone slip rockburst event of May 31, 2015.



Figure 4. Shear plane exposed after the intense rockburst of May 31, 2015.

Following are some details from a few days before main event. On May 21, 2015, a low intensity rockburst, resulted in rock fall above the shield of the cutter head, occurred at chainage 09+758. Another event happened on May 23, 2015 with a moderate rockburst that occurred at chainage 09+742 with a great sound heard from L1 (an area 5 m behind the tunnel face) to the main control room in the cutter head. The third event happened on May 25, 2015 with a slight rockburst near chainage 09+729, which resulted in the fall of fresh rock beyond the shield. On May 26, 2015 multiple, popping sounds were heard near chainage 09+722 beyond the shield. The surrounding rocks deformed, and a lot of fresh rock fell in section L1. It was judged as a minor rock-burst. On May 29, 2015, during excavation a rockburst happened with loud sounds from chainage 09+721 to 09+722, and rock fell in sections L1 and L2 (55 m behind the tunnel face). The great sound of the rockburst was also heard in TBM 697 (left tunnel) at the same time. A rockburst happened once again with a huge sound after some time. A lot of fresh rock also fell beyond the shield. This was judged to be a medium rockburst. Finally, on May 31, 2015 at 11:35 PM, an intense rockburst occurred with a great sound from chainage 09+706 to 09+793 at a depth of 1300 m. This event created deep damage pits in the tunnel and the area near chainage 9+751 received the maximum impact of this final rockburst as shown in Figure 5.

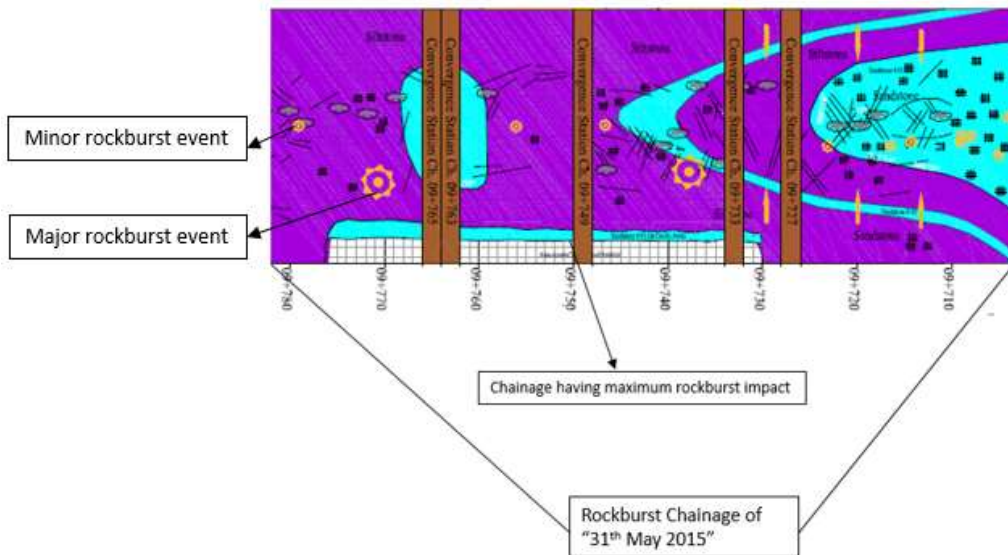


Figure 5. Geological map of the right tunnel, showing the abnormal geology.

Three workers died, and a few others were injured in the May 31, 2015 event. Additionally, a large area of crown and walls fell as shown in Figure 6. Owing to the instant impact of the rock shock, all support systems were destroyed, wire-mesh and ring beams were deformed, and TBM was destroyed. A space of about 30 m behind the cutter head was buried in debris. The total volume collapsed was more than 400

cubic meters. The seismic events before and during the rockburst were recorded using microseismic monitoring equipment, which indicated a Richter magnitude of 2.0. The severe damage indicates the concentration of stresses in this area due to the presence of geological structure. After this big event, the rockburst shockwave caused damage to the left wall and crown of the nearby headrace tunnel (left tunnel) already excavated by TBM 697.



Figure 6. Rockburst damage from the May 31, 2015 event.

After this event, a shear plane was exposed on the boundary of the tunnel, shown in Figure 4. It is concluded here that the series of small rockburst events before the main event paved the way for the final displacement along the exposed shear zone. Those small events were due to brittle failure of hard rock. Asperities along shear zone in high stress environment, which finally caused slippage along this plane and resulted in the most hazardous rockburst event on May 31, 2015, releasing a huge amount of energy. This is very similar to the fault-slip rockburst in the headrace tunnel of the Tianshengqiao II hydropower station [36] and drainage tunnels of the Jinping II hydropower station [35].

6. Numerical Simulation of Shear Zone

Rockburst is a dynamic phenomenon that involves accumulation of huge amounts of energy when structure planes like shear zones are present. To assess the influence of the shear zone on the stability of the NJHPP tunnel and for better understanding of the rockburst failure mechanism around the tunnels, we performed a FLAC3D numerical simulation. From the known massive hard rock geology, it was obvious to choose the FLAC3D continuum model to find the influence of the shear zone on the stability of the tunnel. The field observations revealed a shear zone exposed after intense rockburst, as shown in Figure 4.

This shear zone was nearly perpendicular to the right tunnel axis [31]. To find the reason behind the intense rockburst event, a shear zone was simulated perpendicular to the right-side tunnel axis. The size of the model is 127 m × 100 m × 100 m, as shown in Figure 7. The two blocks of 50 m each were created and named Front and Back block. The shear zone is modelled as interface zone between the two blocks. Elasto-Plastic material model with Mohr-Coulomb criteria is used for the analysis. A model with sandstone rock unit parameters was simulated to check the effect of shear zone on rock mass and tunnel.

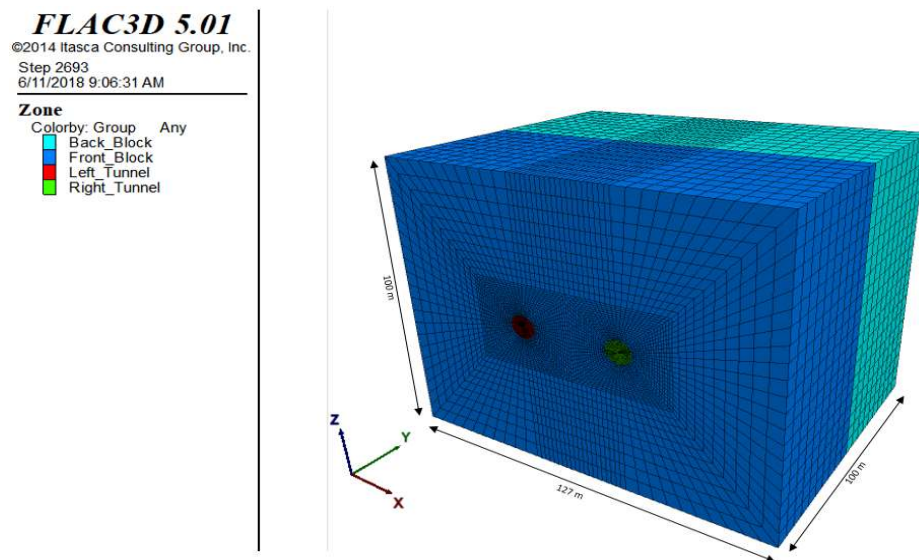


Figure 7. Rock mass model

The twin tunnels, each with diameter 8.53 m, were simulated according to the actual construction sequence, as shown in Figure 7. The center to center distance between these twin tunnels is 33 m. Compressive strength of intact rock (σ_{ci}), geological strength index (GSI), rock intact modulus (E_i), and material constant (mi) were used to find the mechanical parameters of sandstone for different rock covers. The average values of the stresses were applied in three directions according to over-coring results. The maximum principal stress (σ_{xx}) with a value of 60 MPa, intermediate principal stress (σ_{yy}) with a value of 37 MPa, and minimum principal stress (σ_{zz}) with a value of 35 MPa were applied in the FLAC three-dimensional model. Three different types of mesh primitive shapes (radtunnel, radcylinder, brick) were connected together. The model has 113600 zones. Fine mesh was simulated around the twin tunnels to get better results near the boundary of excavation. After simulating the geometric model, reasonable boundary conditions were applied, all sides of the model were fixed, except the top side to apply vertical stresses (σ_{zz}). The following table shows the mechanical properties of the rock mass applied during the numerical modeling.

Table 2. Mechanical parameters of the rock mass.

Rock Type	Young's modulus (GPa)	Poisson's ratio (ν)	Cohesive Strength (MPa)	Friction angle ($^\circ$)	Depth(m)
Sandstone	20	0.25	4.2	42	1300

6.1. Interface Element

FLAC3D provides an interface element to represent structures like the shear zone in a geologic medium. This element is a collection of triangular elements. It can be created at any location in the model. In our model, the interface element is attached to a front block at 50 m length in the right headrace tunnel to reflect the actual field conditions as shown Figure 8. After creating the interface element, the space between the front and back block is removed and back block is moved 1m back to get attach with the front block. Both blocks are attached without attaching the shear zone area. Interface element is characterized by Coulomb sliding. Shear displacement causes an increase in the effective normal stress on the interface during sliding. Different parameters like normal stiffness (K_n) and shear stiffness (K_s), friction angle ($^\circ$), cohesion (MPa), dilation (ψ) and tensile strength (MPa) are usually assigned to interface element. In this analysis the values were $K_n=5.4\times 10^4$ Pa and $(K_s)=2.4\times 10^4$ Pa for normal and shear stiffness of interface element respectively [37]. Low values of friction angle and cohesion were used to reflect the worse scenario. The value of cohesion was selected as zero and the friction angle was 5° [38].

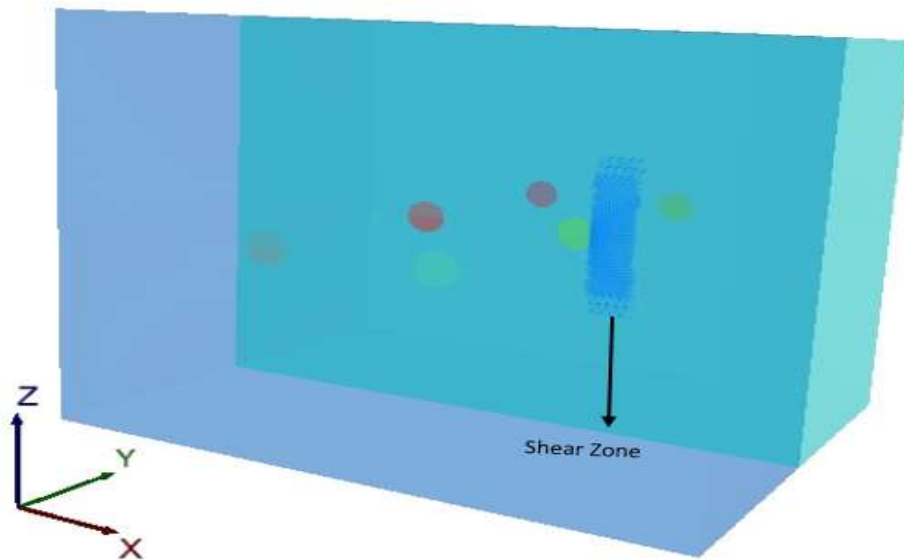
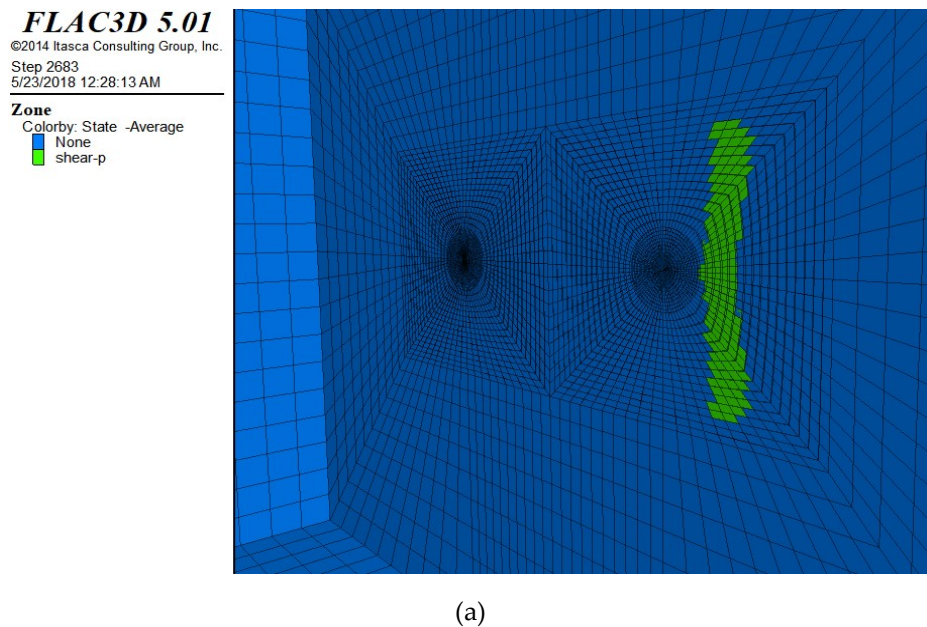


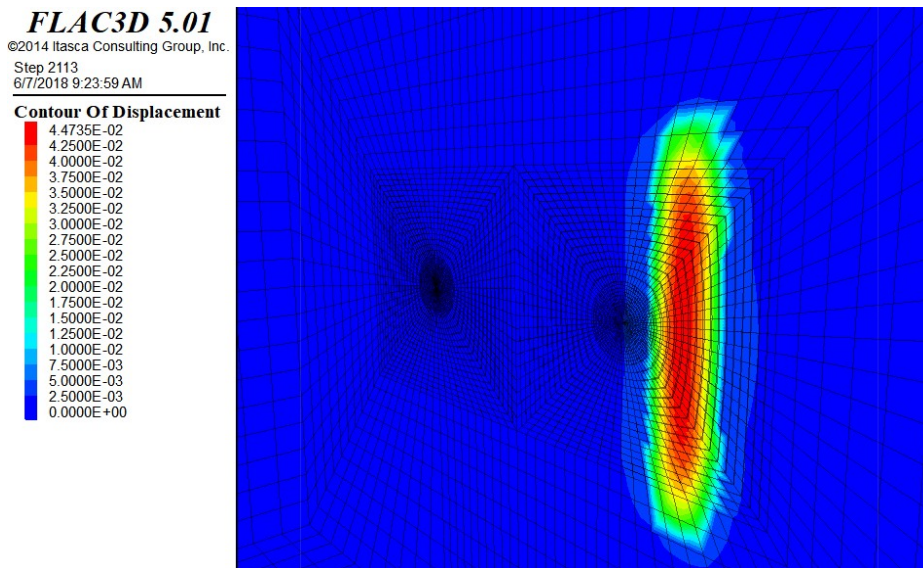
Figure 8. FLAC3D model with shear zone.

7. Results of Numerical Analysis

7.1. Initial conditions

The FLAC3D code is used to simulate the stress and deformation of rock materials under loading conditions. The shear zone was successfully simulated with this software to study the danger of rockburst. The simulated model was run after applying the initial conditions. As we discussed in Sec.1, the shear zone acts as a barrier and the stresses are usually concentrated there. When a shear zone is present in abnormal geological conditions, it is a more dangerous condition for rockburst as shown in Figure 5. The FLAC3D model was run after applying initial conditions. The model shows that the shear zone was in a shear state and showing some displacement before the start of the excavation, see Figure 9(a). The displacement of 44.7 mm can also be seen in the Figure 9(b).

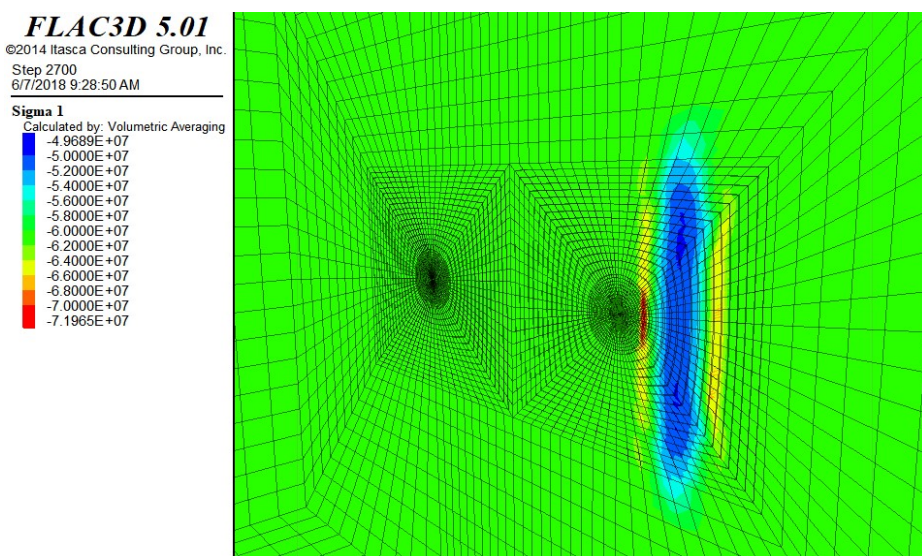




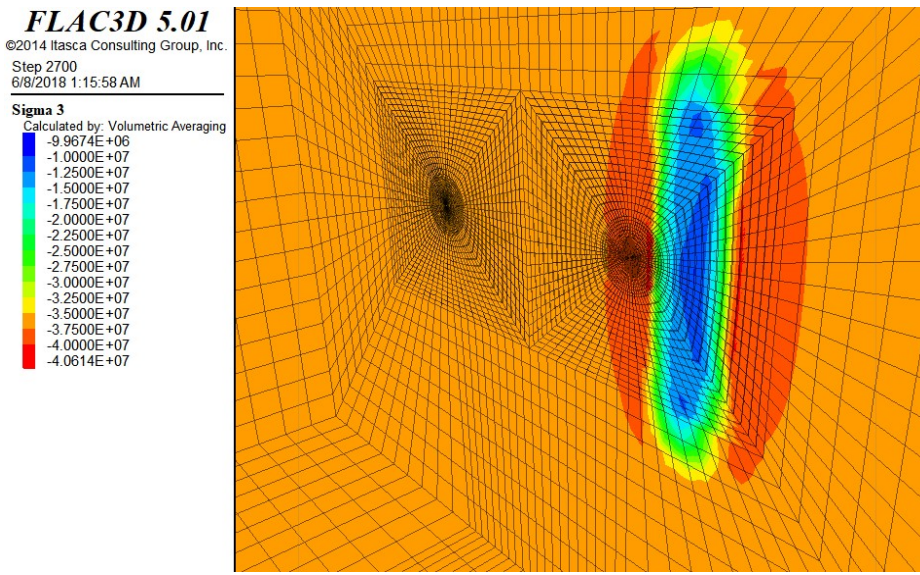
(b)

Figure 9. (a) Zone state in the shear zone area and (b) contour of the displacement in the shear zone area.

Contours of maximum and minimum principal stresses show stress concentration in the shear zone area on the right side of the right headrace tunnel because there is no such stress concentration in any other region of the model as shown in Figure 10 (a) and (b). Notably, the maximum stress occurs near the right tunnel. The shear stress has maximum concentration in the area where the structural plane is present as shown in figure 11. As can be seen, the minimum shear stress is 10 MPa near the boundary of the shear zone whereas maximum shear stress occurs in the middle of shear zone with a magnitude of 21.5 MPa.



(a)



(b)

Figure 10. Principal stress concentration during initial condition:

(a) contour of maximum principal stress and (b) contour of minimum principal stress.

Numerical simulation has also given promising results regarding the displacement near the shear zone before excavation. This reflects that the shear zone is a disturbed area, which was displaced before excavation as shown in the figure 9(b) and have a very high chance of shear slip movement when the tunnel will be excavated through this zone. Figure 11 shows the contour map of the shear stress inside and near the shear zone.

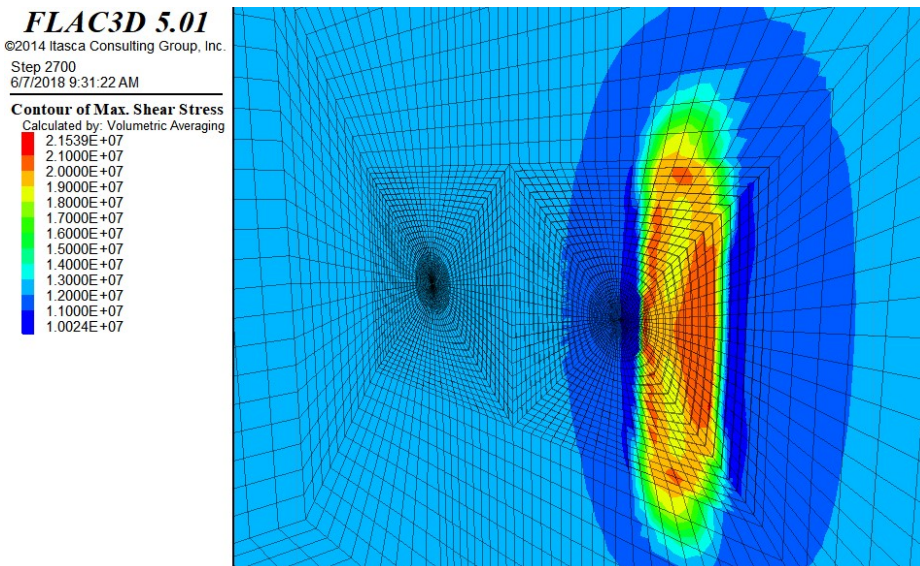
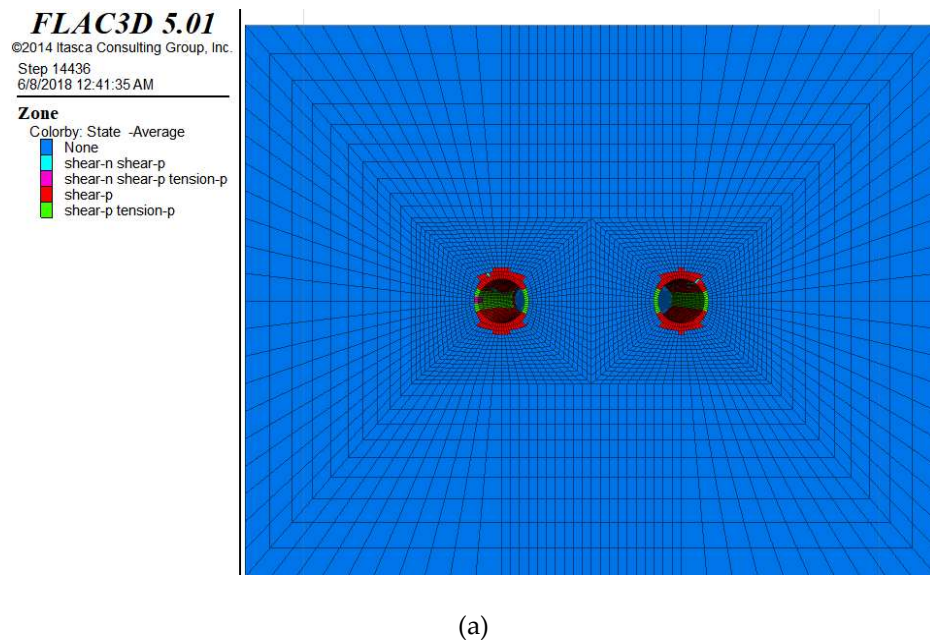


Figure 11. Contour of the maximum shear stress concentration for the initial condition.

7.2. Excavation Stage

The headrace tunnels in the NJHPP were excavated by both the drill-and-blast method and the TBM method. The portion of the tunnel that was affected by the intense rockburst was excavated by TBM, which has very little flexibility during construction. The behavior of the rock mass and tunnel after excavation is shown in Figure 12. The average zone state along the tunnel profile shows a shear state (shear-p) on the crown and invert, while the wall of the tunnel is in a mixed shear and tension state (shear-p and tension-p). Figure 12(b) shows the excavated area of both tunnels. As the excavation process approaches the shear zone, the tunnel is in a state of both shear and tension (shear-p tension-p), which further intrudes into the shear zone, present perpendicular to the axis of the right tunnel, as shown in Figure 12(b). This shows that the zone state extended its influence beyond the boundary of the tunnel. This unstable area, under the influence of high stresses, caused a shear slip in the shear zone area, which finally resulted in a release of huge amounts of energy in the form of the rockburst.



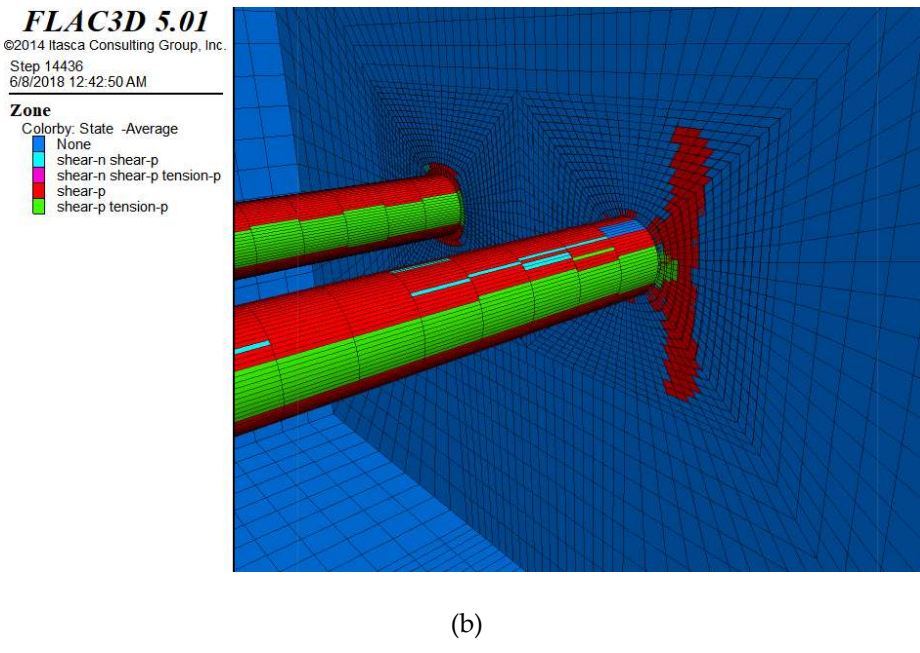
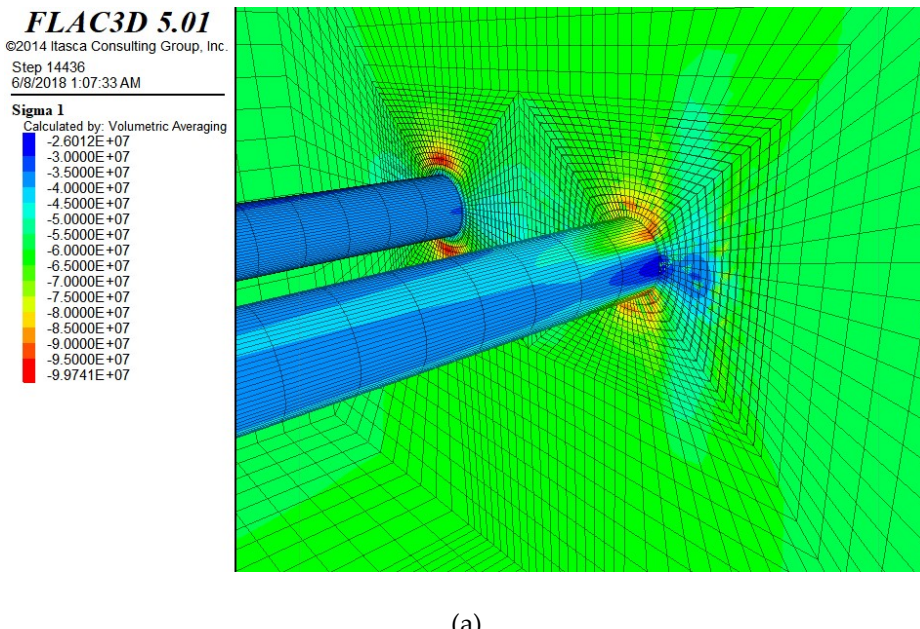
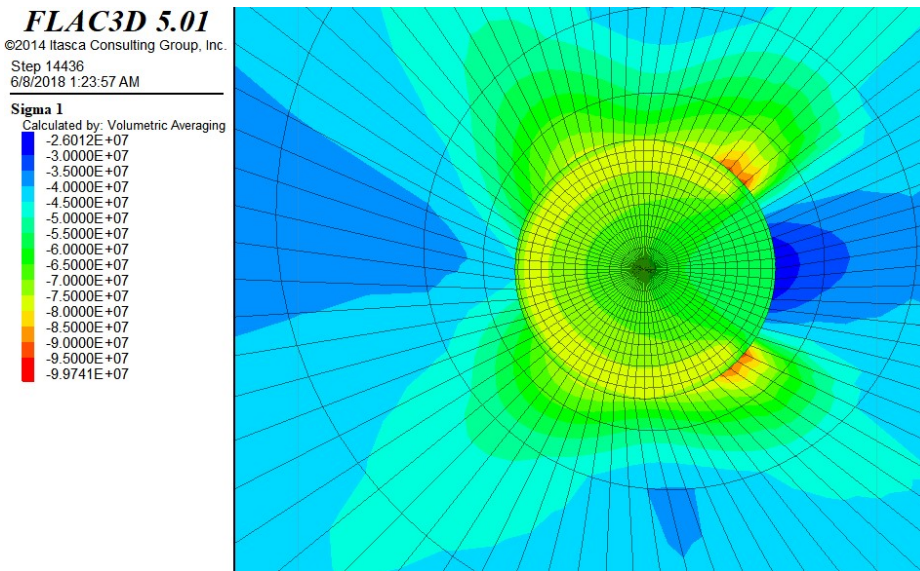


Figure 12. Zone state after excavation stage: (a) cross-sectional view and (b) longitudinal view.

During normal conditions, horizontal stress is the maximum principal stress, therefore, its concentration should be high at the crown and invert level. The contours of the maximum principal stress show a normal situation i.e. the stress contour migrates from the left tunnel periphery (Figure.13(a)). However, due to the influence of the shear zone in the right tunnel, the contours of maximum principal stress is near the periphery of the tunnel shown in Figure.13(b). The Concentration of maximum principal stress on the face of right hand tunnel can be seen in figure 13(b).

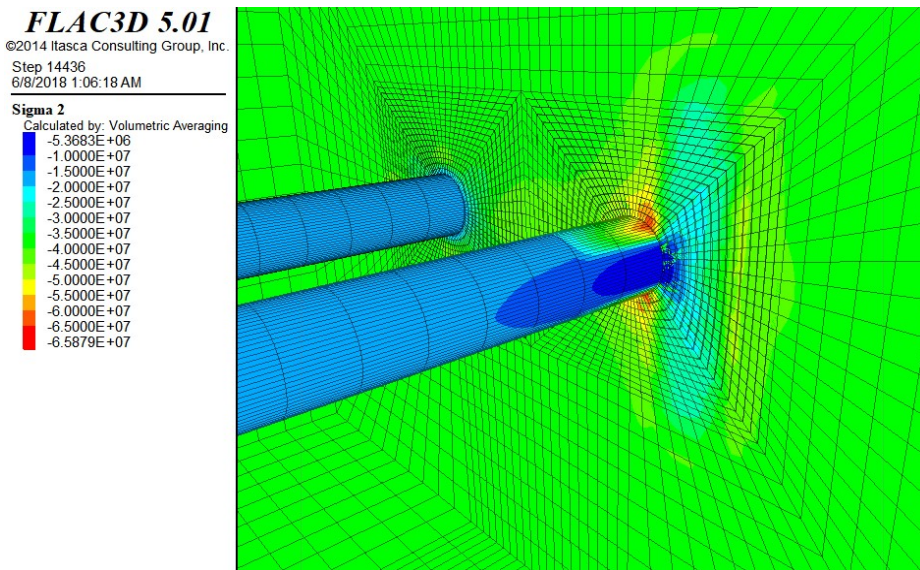




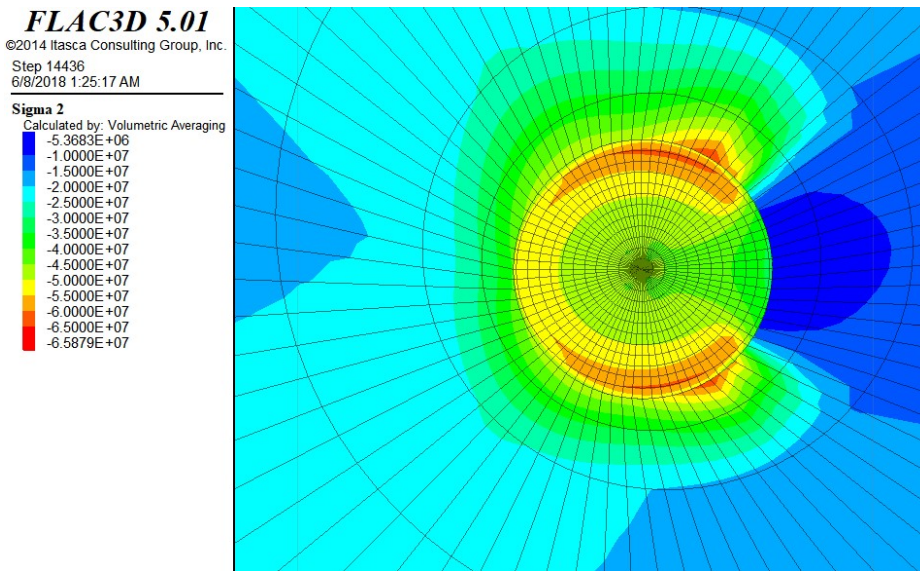
(b)

Figure 13. contours of maximum principal stress: (a) in twin tunnels and (b) on the face of right tunnel

The intermediate principal stress is usually ignored during 2D stress analysis, but it cannot be ignored when the maximum principal stress is in the horizontal direction [39]. At the face of the tunnel, the FLAC3D numerical simulation shows that the intermediate principal stress is concentrated at the crown and invert level on the right tunnel as shown in figure 14(a). On the face of right tunnel impact of shear zone on intermediate principal stress can also be seen in figure 14(b) which makes conditions favorable for rock burst.



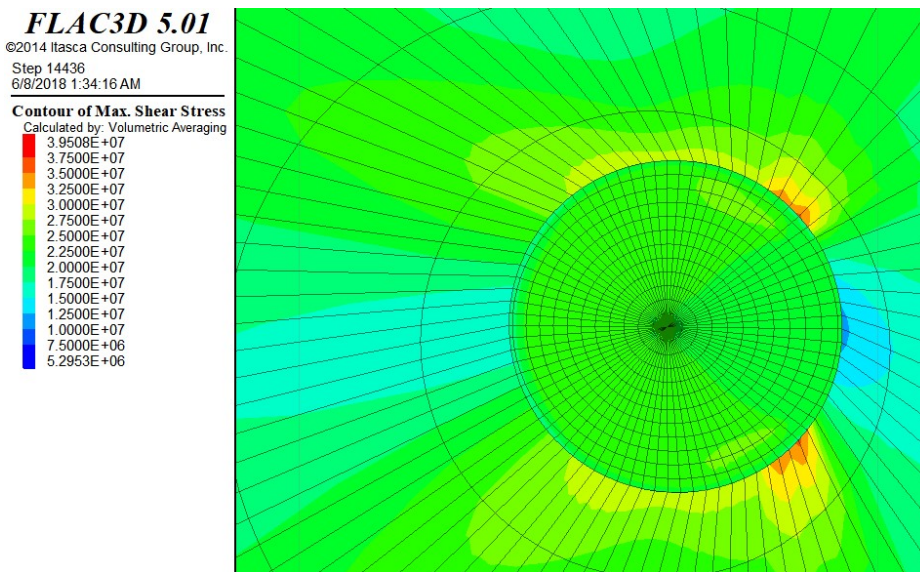
(a)



(b)

Figure 14. contours of intermediate principal stress: (a) in twin tunnels and (b) on the face of right tunnel

The shear zone has a significant impact on shear stress. Therefore, numerical simulation results have shown shear stress concentration near the shear zone in right tunnel face area as shown in Figure 15(a.) and displacement due to induced stresses is shown in figure 15(b).



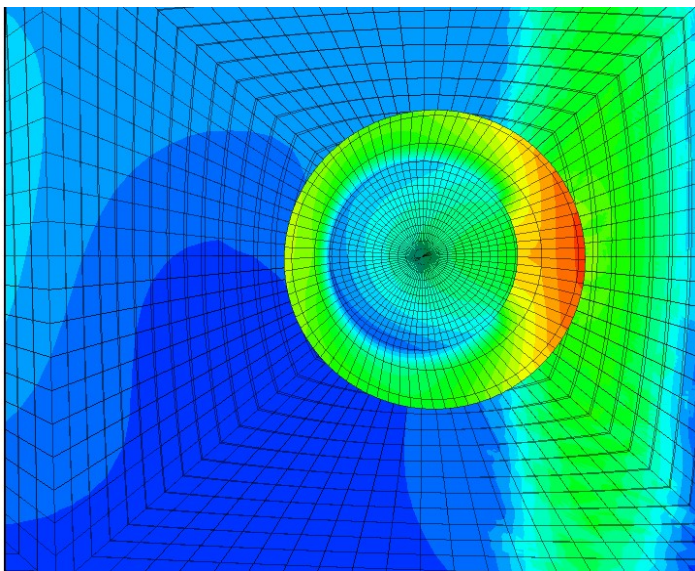
(a)

FLAC3D 5.01

©2014 Itasca Consulting Group, Inc.
Step 14741
5/3/2018 9:47:30 AM

Contour Of Displacement

9.7513E-02
9.0000E-02
8.0000E-02
8.5000E-02
7.5000E-02
7.0000E-02
6.5000E-02
6.0000E-02
5.5000E-02
5.0000E-02
4.5000E-02
4.0000E-02
3.5000E-02
3.0000E-02
2.5000E-02
2.0000E-02
1.5000E-02
1.0000E-02
5.0000E-03
0.0000E+00



(b)

Figure.15. contour of: (a) maximum shear stress after excavation and (b) displacement after excavation

It is evident from the previous results (Figure.13-15(a)) that there is a concentration of principal stresses near the shear plane that caused displacement in the shear zone when the excavation approaches this area as shown in Figure.15(b). During this excavation stage, shear stress and shear displacement is produced in shear zone that is shown in figure 16(a) and (b). The shear stresses are concentrated where the shear zone approaches the wall of right tunnel. The results of normal and normal displacement in the shear zone is shown in Figure.17 (a) and (b).

FLAC3D 5.01

©2014 Itasca Consulting Group, Inc.
Step 14436
6/8/2018 9:40:18 AM

Shear Zone Shear Stress

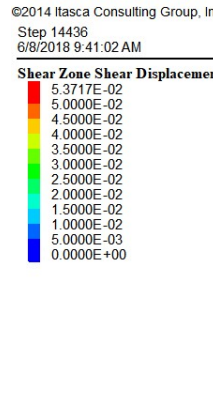
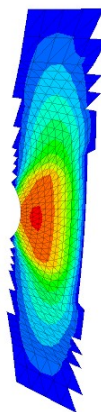
5.0712E+02
5.0000E+02
4.5000E+02
4.0000E+02
3.5000E+02
3.0000E+02
2.5000E+02
2.0000E+02
1.5000E+02
1.0000E+02
5.0000E+01
0.0000E+00

FLAC3D 5.01

©2014 Itasca Consulting Group, Inc.
Step 14436
6/8/2018 9:41:02 AM

Shear Zone Shear Displacement

5.3717E-02
5.0000E-02
4.5000E-02
4.0000E-02
3.5000E-02
3.0000E-02
2.5000E-02
2.0000E-02
1.5000E-02
1.0000E-02
5.0000E-03
0.0000E+00



(a)

(b)

Figure.16. contour shear zone: (a) shear stress and (b) shear displacement

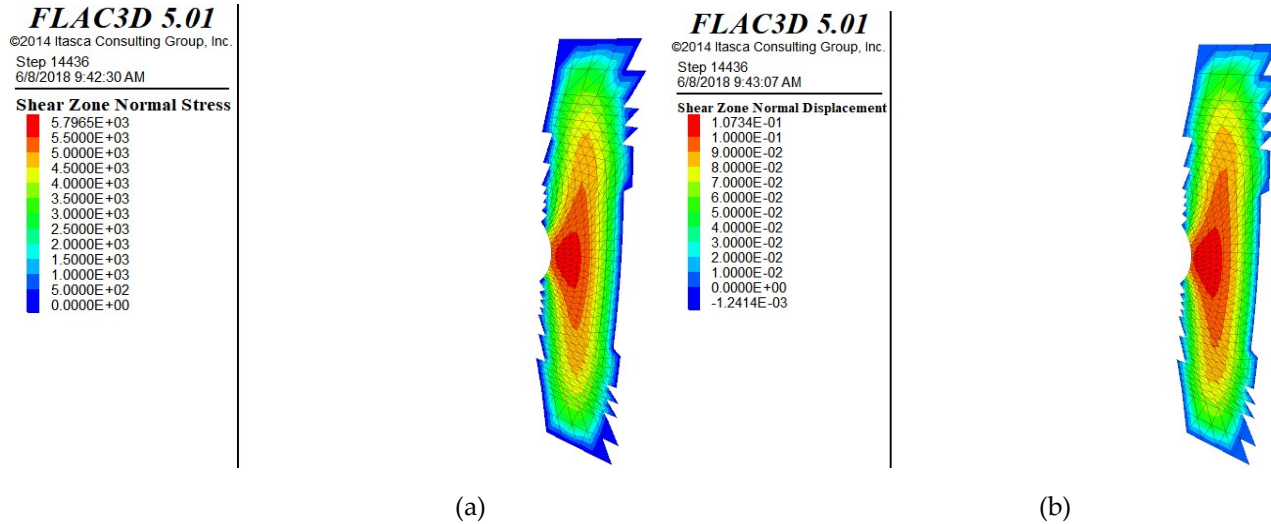


Figure 17. contour shear zone: (a) normal stress and (b) normal displacement

8. Discussion

The role of the shear zone as an in-situ stress-concentrating barrier is studied with the three-dimensional numerical simulation via FLAC3D. The impact of the shear zone in deep NJHPP tunnel is studied which has a high stress regime due to tectonics and the maximum principal stress is in the horizontal direction. Because of this high stress concentration, an intense rockburst event occurred near the shear zone during the construction of the project. Rockburst event of May 31, 2015 is specifically studied and numerical simulation is used to find the mechanism behind this event. A nearly vertical shear zone was exposed after the rockburst events in the right tunnel. In this section, the effect of the shear zone on the behavior of tunnels and rock mass is discussed both before the excavation as well as during excavation stage.

The conditions before the excavation are studied first. Figure 9a shows that the shear zone is already in a shear state even before the excavation started, which shows the presence of a shear zone is favorable to failure. The right tunnel has more favorable condition for failure as compared to left tunnel where no shear zone is present in the vicinity. Rock mass is also displaced before the excavation. This displacement is maximum in the center of shear zone and minimum at boundaries as shown in figure 9b. The maximum value of the displacement is 44.7 mm. Stresses are concentrated near the shear zone and figure 10 shows maximum and minimum principal stress concentration in rock mass. Near the shear zone, the maximum and the minimum principal stresses has a magnitude of 71.9 MPa and 40.6 MPa respectively while rest of rock mass has applied stress conditions. The contour map of maximum shear stress in rock mass after

applying initial conditions have maximum value of 21.5 MPa in the center of shear zone. Therefore, after applying initial conditions it is evident that the area near stressed shear zone has very high chances of movement in shear along shear plane.

The zone states, principal stresses, and displacements in the shear zone were studied after excavating the tunnels. The zone state was used to check whether the stresses of the rock mass zones around the tunnel satisfy the yield criterion. The twin tunnels are in a shear and tension states at the walls and are totally in shear at the crown and invert level, which is due to the high in-situ stresses, as shown in Figure 12a. The zone states extend into the shear zone area while there is no such intrusion in the left tunnel as shown in longitudinal view of twin tunnels. The shear zone is completely in the shear state and huge amounts of stored strain energy is released from rockburst in this region. Because of the abnormal stress conditions, the boundary of the tunnel is in both a shear and tension state. There is no such stress concentration in left tunnel. During excavation stage, is increased in the form of tangential stresses having the maximum value of 99.7 MPa is concentrated to the tunnel crown and invert as shown in Figure.13a. In the right tunnel, the maximum principal stress has its concentration along the periphery of the tunnel while it is concentrated away in left tunnel. The result of this high stress concentration along the periphery increases the risk of rockburst in the right tunnel. The stress concentration in the right tunnel face has also confirmed the risk of rockburst there. The intermediate principal stress has a high value when the tunnel reaches the shear zone. It is concentrated at the crown and invert level of the tunnel and have maximum value of 65 MPa as shown in figure.14(a) and (b). In case of rock burst, the intermediate principal stress also contributed to the abnormal stress concentration in the area which finally resulted in rock burst. This stress concentration has caused the maximum displacement of 97.5 mm when the tunnel approaches the shear zone which has maximum shear stress value of 39.5 MPa. Finally, the Interface element reflects the shear zone in FLAC3D. The shear and the normal stresses are concentrated in the middle of the shear zone where maximum shear and normal displacement have occurred. When the excavation is reached near the shear zone, the shear displacement reaches to the maximum value of 53.7 MM there.

Therefore, there is a close relationship between high in-situ stress, shear zone, and rockburst. The presence of a shear zone type geological structure in high stress environment makes the conditions ideal for sudden shear failure, which releases huge amounts of energy in the form of rockburst.

9. Conclusion

This study investigated the impact of a shear zone on rockburst in deep hydropower tunnels. The effect of the structural plane on rockburst was studied first. Then, the FLAC3D simulation was used to study this problem numerically. A FLAC3D model with the representative rock mass and twin tunnels was built with a Mohr-Coulomb constitutive model. The simulation procedure involved initial conditions analysis and post-excavation stage analysis. The relationship between high in-situ stress, shear zone, and rockburst was explored. The following conclusions were obtained from this study:

1. The shear zone acts as barrier for stress accumulation, which suddenly releases in the form of a rockburst. The amount of energy stored depends on the in-situ stress conditions, the presence of a shear zone, and rock type. Hard rock, which store more energy due to its high modulus of elasticity, results in an intense rockburst in the presence of a nearby shear zone.

2. The location of the May 31, 2015 rockburst event was near abnormal geological settings, where the bedding plane becomes horizontal due to the concentration of high stresses. These high stresses are the reason behind the aforementioned rockburst.
3. A FLAC3D numerical simulation validated the results that were established theoretically. In the high stress regime, the principal stresses were concentrated near the shear zone. The rock mass showed displacement even before the start of the excavation, which reflects that the shear zone area is the most susceptible to rockburst.
4. After excavation, the shear zone showed more shear displacement, which is the main reason behind the intense rockburst of May 31, 2015 in the right headrace tunnel. Furthermore, the excavation in the nearby left tunnel was smooth, without any rockburst event, which reflects the impact of the shear plane in the right tunnel.
5. It can be concluded that the presence the shear zone, high stress concentration, and complex geological settings worked together and produced the dangerous condition for the May 31, 2015 event, which resulted in a great loss of human life and property.

Acknowledgments: This study was supported by the Development of Design and Construction Technology for Double Deck Tunnel in Great Depth Underground Space (17SCIP-B089409-04) from Construction Technology Research Program funded by Ministry of Land, Infrastructure and Transport of the Korean government. The authors (Abdul Muntaqim Naji and Hafeezur Rehman) are extremely thankful to the Higher Education Commission (HEC) of Pakistan for HRDI-UESTPs scholarship.

Author Contributions: Hankyu Yoo supervised the research. Abdul Muntaqim Naji has developed the proposed research concept. Muhammad Zaka Emad made important suggestions and recommendations. Hafeezur Rehman helped in writing and re-checking the paper technically as well as grammatically.

Conflicts of Interest: The authors declare no conflict of interest.

References:

1. Tang, B., *Rockburst control using destress blasting*. 2000, McGill University Montreal.
2. Kaiser, P.K., *Canadian rockburst support handbook*: 1996. 1996: Geomechanics Research Centre.
3. Liu, X., et al., *Time Effect of Water Injection on the Mechanical Properties of Coal and Its Application in Rockburst Prevention in Mining*. Energies, 2017. **10**(11): p. 1783.
4. Vižintin, G., M. Kocjančič, and M. Vulić, *Study of coal burst source locations in the velenje colliery*. Energies, 2016. **9**(7): p. 507.
5. Drzewiecki, J. *Coal Mining in Poland in Complicated Geological Conditions*. in *proceedings International Conference of Clean Coal as a Sustainable Energy development Strategy*. 2003.
6. Butra, J. and J. Kudełko, *Rockburst hazard evaluation and prevention methods in Polish copper mines*. 2011.
7. Zhao, H. and R.B. Kaunda, *Numerical Assessment of the Influences of Gas Pressure on Coal Burst Liability*. Energies, 2018. **11**(2): p. 260.
8. Jack Mierzejewski, G.P., Bruce Ashcroft, *Short-Term Rockburst Prediction in TBM Tunnels*, in *World Tunnel Congress*. 2017: Bergen, Norway. p. 10.
9. Shan, Z.-g. and P. Yan, *Management of rock bursts during excavation of the deep tunnels in Jinping II Hydropower Station*. Bulletin of Engineering Geology and the Environment, 2010. **69**(3): p. 353-363.

10. Zhou, H., et al., *Analysis of rockburst mechanisms induced by structural planes in deep tunnels*. Bulletin of engineering geology and the environment, 2015. **74**(4): p. 1435-1451.
11. Hagedorn, H., M. Rehbock-Sander, and R. Stadelmann. *Gotthard Base tunnel: rock burst phenomenon during construction of a multifunctional section in a fault zone area*. in *11th ISRM Congress*. 2007. International Society for Rock Mechanics.
12. Kaiser, P.K. and M. Cai, *Design of rock support system under rockburst condition*. Journal of Rock Mechanics and Geotechnical Engineering, 2012. **4**(3): p. 215-227.
13. Reddy, N. and S. Spottiswoode, *The influence of geology on a simulated rockburst*. JOURNAL-SOUTH AFRICAN INSTITUTE OF MINING AND METALLURGY, 2001. **101**(5): p. 267-274.
14. Zhang, C., et al., *Rockmass damage development following two extremely intense rockbursts in deep tunnels at Jinping II hydropower station, southwestern China*. Bulletin of engineering geology and the environment, 2013. **72**(2): p. 237-247.
15. Jiayou, L., et al. *The brittle failure of rock around underground openings*. in *ISRM International Symposium*. 1989. International Society for Rock Mechanics.
16. Amadei, B. and O. Stephansson, *Rock stress and its measurement*. 1997: Springer Science & Business Media.
17. Shepherd, J., L. Rixon, and L. Griffiths. *Outbursts and geological structures in coal mines: a review*. in *International Journal of Rock Mechanics and Mining Sciences & Geomechanics Abstracts*. 1981. Elsevier.
18. Hedley, D.G., *Rockburst handbook for Ontario hardrock mines*. 1992: Canmet.
19. Ortlepp, W. and T. Stacey, *Rockburst mechanisms in tunnels and shafts*. Tunnelling and Underground Space Technology, 1994. **9**(1): p. 59-65.
20. Durrheim, R., et al., *Factors influencing the severity of rockburst damage in South African gold mines*. JOURNAL-SOUTH AFRICAN INSTITUTE OF MINING AND METALLURGY, 1998. **98**: p. 53-58.
21. Ortlepp, W., *Observation of mining-induced faults in an intact rock mass at depth*. International Journal of Rock Mechanics and Mining Sciences, 2000. **37**(1-2): p. 423-436.
22. Jiang, Q., et al., *Rockburst characteristics and numerical simulation based on a new energy index: a case study of a tunnel at 2,500 m depth*. Bulletin of engineering geology and the environment, 2010. **69**(3): p. 381-388.
23. Snelling, P.E., L. Godin, and S.D. McKinnon, *The role of geologic structure and stress in triggering remote seismicity in Creighton Mine, Sudbury, Canada*. International Journal of Rock Mechanics and Mining Sciences, 2013. **58**: p. 166-179.
24. Feng, X., et al., *Mechanism, warning and dynamic control of rockburst development processes*. China Social Sciences Publishing House, 2013.
25. Manouchehrian, A. and M. Cai, *Analysis of rockburst in tunnels subjected to static and dynamic loads*. Journal of Rock Mechanics and Geotechnical Engineering, 2017. **9**(6): p. 1031-1040.
26. Qiao, C. and Z. Tian, *Study of the possibility of rockburst in Dongguan-shan Copper Mine*. Chinese J. Rock Mech. Eng. Žexp, 1998. **17**: p. 917-921.
27. Grimstad, E. *Updating the Q-system for NMT*. in *Proceedings of the International Symposium on Sprayed Concrete-Modern use of wet mix sprayed concrete for underground support, Fagernes, Oslo, Norwegian Concrete Association*, 1993. 1993.
28. Barton, N., R. Lien, and J. Lunde, *Engineering classification of rock masses for the design of tunnel support*. Rock mechanics, 1974. **6**(4): p. 189-236.
29. Sharma, M. and D. Shanker, *Estimation of seismic hazard parameters for the Himalayas and its vicinity from mix data files*. ISET J Earthq Technol, 2001. **38**(2-4): p. 93-102.
30. Bieniawski, Z.T. and Z. Bieniawski, *Engineering rock mass classifications: a complete manual for engineers and geologists in mining, civil, and petroleum engineering*. 1989: John Wiley & Sons.
31. Bawden, W.F. *Neelum Jhelum Hydroelectric Project Rockburst Investigation Report*. 2015.

32. Wang, C. and L. Bao, *Predictive analysis of stress regime and possible squeezing deformation for super-long water conveyance tunnels in Pakistan*. International Journal of Mining Science and Technology, 2014. **24**(6): p. 825-831.
33. Wang, J.-A. and H. Park, *Comprehensive prediction of rockburst based on analysis of strain energy in rocks*. Tunnelling and Underground Space Technology, 2001. **16**(1): p. 49-57.
34. Zhao, Z.N., *Studies on preparation causes of rockburst in Deep Tunnel Based on Microseismic information*. 2013.
35. Zhang, C., et al., *Case histories of four extremely intense rockbursts in deep tunnels*. Rock mechanics and rock engineering, 2012. **45**(3): p. 275-288.
36. Lee, C., W. Sijing, and Y. Zhifu, *Geotechnical aspects of rock tunnelling in China*. Tunnelling and Underground Space Technology, 1996. **11**(4): p. 445-454.
37. Group, I.C., *FLAC3D 5.0 manual*. 2012, Itasca Consulting Group Minneapolis.
38. Elhami, E., *2D Modeling of Kristineberg Mine Stope: A Parameter Study*. 2011.
39. Eberhardt, E., *Numerical modelling of three-dimension stress rotation ahead of an advancing tunnel face*. International Journal of Rock Mechanics and Mining Sciences, 2001. **38**(4): p. 499-518.